

University of Groningen

## Ultralow Power Microfuses for Write-Once Read-Many Organic Memory Elements

de Brito, Bianca C.; Smits, Edsger C. P.; van Hal, Paid A.; Geuns, Tom C. T.; de Boer, Bert; Lasance, Clemens J. M.; Gomes, Henrique L.; de Leeuw, Dago M.; Hal, Paul A. van

*Published in:*  
Advanced Materials

*DOI:*  
[10.1002/adma.200800960](https://doi.org/10.1002/adma.200800960)

**IMPORTANT NOTE:** You are advised to consult the publisher's version (publisher's PDF) if you wish to cite from it. Please check the document version below.

*Document Version*  
Publisher's PDF, also known as Version of record

*Publication date:*  
2008

[Link to publication in University of Groningen/UMCG research database](#)

*Citation for published version (APA):*

de Brito, B. C., Smits, E. C. P., van Hal, P. A., Geuns, T. C. T., de Boer, B., Lasance, C. J. M., ... Hal, P. A. V. (2008). Ultralow Power Microfuses for Write-Once Read-Many Organic Memory Elements. *Advanced Materials*, 20(19), 3750-+. DOI: 10.1002/adma.200800960

**Copyright**

Other than for strictly personal use, it is not permitted to download or to forward/distribute the text or part of it without the consent of the author(s) and/or copyright holder(s), unless the work is under an open content license (like Creative Commons).

**Take-down policy**

If you believe that this document breaches copyright please contact us providing details, and we will remove access to the work immediately and investigate your claim.

*Downloaded from the University of Groningen/UMCG research database (Pure): <http://www.rug.nl/research/portal>. For technical reasons the number of authors shown on this cover page is limited to 10 maximum.*

# Ultralow Power Microfuses for Write-Once Read-Many Organic Memory Elements\*\*

By Bianca C. de Brito, Edsger C. P. Smits, Paul A. van Hal, Tom C. T. Geuns, Bert de Boer, Clemens J. M. Lasance, Henrique L. Gomes, and Dago M. de Leeuw\*

Organic integrated circuits are being developed for application in contactless radio-frequency identification (RFID) transponders.<sup>[1,2]</sup> The largest reported digital integrated circuit is a functional 64-bit code generator comprising about 2000 organic field-effect transistors.<sup>[1]</sup> The digital code was stored in a hardwired, or Mask-ROM, memory matrix. Envisaged high-end applications will require dynamic memories that can repeatedly be written and read. Many low-end applications however, such as electronic barcodes, require only static memory elements that can be written once and read many times (WORM). For these WORM applications, electrically programmable read-only memory elements based on conducting polypyrrole<sup>[3]</sup> and polyaniline lines<sup>[4]</sup> have been developed. The operating mechanism relies on the irreversible reduction of the electrical conductivity of polyaniline by Joule heating, similar to standard safety fuses. The critical power for fuse interruption was found to be independent of the line width and directly proportional to the line length.<sup>[4]</sup> The breakdown is current driven and about 0.5 mW was needed to blow up the shortest lines of 5  $\mu\text{m}$ . The power to blow up a single fuse can be delivered by state-of-the-art organic integrated circuits. However, the critical power is too large to program memory arrays. To minimize power consumption the line width has to be reduced. To this end the layout was changed from a lateral

to a vertical fuse by sandwiching the conducting polymer, poly(3,4-ethylene-dioxythiophene) stabilized with polystyrene sulfonic acid (PEDOT/PSS), between two electrodes. Integration of PEDOT/PSS in cross-bar memory arrays with silicon diodes has been reported.<sup>[5]</sup> High voltage pulses were needed to program the memory. Current-controlled thermal dedoping of PEDOT/PSS was postulated as an operation mechanism. Here we show that the vertical PEDOT/PSS fuses can be programmed with ultralow-power of only a few  $\mu\text{W}$ . We show that the operating mechanism is not dedoping by Joule heating but delamination by gas formation upon electrolysis of water. To unambiguously demonstrate that fuse interruption is voltage- and not power-driven, breakdown of fuses connected in series was investigated.

In order to prevent cross-talk, the PEDOT/PSS fuses were fabricated in vertical interconnect holes (vias) of a lithographically patterned photoresist. Silicon monitor wafers (150 mm) with thermally grown oxide were used as a substrate. Bottom gold electrodes and first interconnects were defined by photolithography. Chromium was used as an adhesion layer. Subsequent via holes with a diameter between 1  $\mu\text{m}$  and 50  $\mu\text{m}$  were defined in 500 nm of the photoresist. After development, baking, and oxygen plasma cleaning, a PEDOT/PSS layer was spin-coated. Various types of PEDOT/PSS were obtained from H.G. Starck and Agfa. The conductivity varied between 0.01  $\text{Scm}^{-1}$  and 100  $\text{Scm}^{-1}$ . A top gold electrode was evaporated and patterned. The top electrode acts as a self-aligned etching mask for the removal of the exposed PEDOT/PSS with reactive ion etching. The fuse geometry is schematically depicted in the inset of Figure 1. Each wafer contained about 500 discrete vertical fuses. Fuses were combined into strings of 20 and 40 fuses in series. The current–voltage characteristics were measured using an Agilent 4155C semiconductor parameter analyzer. There was no difference between two-point and four-point probe current–voltage measurements. Unless stated otherwise the measurements were performed in ambient conditions.

A typical current–voltage measurement is presented in Figure 1. The bias was swept from 0 to 10 V on a logarithmic scale, and the current increased linearly with the bias. However, at a critical voltage of about 2 V the current irreversibly drops by several orders of magnitude. The vertical PEDOT/PSS fuse is blown up. The interruption is independent of polarity and hardly depends on the scan rate that was varied between 5 and 250  $\text{msV}^{-1}$ . Scanning electron microscopy (SEM) photographs before and after the fuse interruption are

[\*] Prof. D. M. de Leeuw, E. C. P. Smits, Dr. P. A. van Hal, T. C. T. Geuns, C. J. M. Lasance

Philips Research Laboratories  
High Tech Campus 4  
5656 AE Eindhoven (The Netherlands)  
E-mail: dago.de.leeuw@philips.com

Prof. D. M. de Leeuw, E. C. P. Smits, Prof. B. de Boer  
University of Groningen  
Zernike Institute of Advanced Materials  
Nijenborgh 4 9747 AG Groningen (The Netherlands)

E. C. P. Smits  
Dutch Polymer Institute (DPI)  
P.O. Box 902  
5600 AX Eindhoven (The Netherlands)

B. C. de Brito, Prof. H. L. Gomes  
Centre of Electronic Optoelectronics and Telecommunications  
Universidade do Algarve  
Campus de Gambelas  
8000 Faro (Portugal)

[\*\*] The authors gratefully acknowledge financial support from the EC (POLYAPPLY IST-IP-507143). The work of E. C. P. S. forms part of the Dutch Polymer Institute (DPI) research program (project no. 516). We thank R. G. R. Weemaes from the materials analysis department of MiPlaza for the FIB measurements. Supporting Information is available online from Wiley InterScience or from the author.

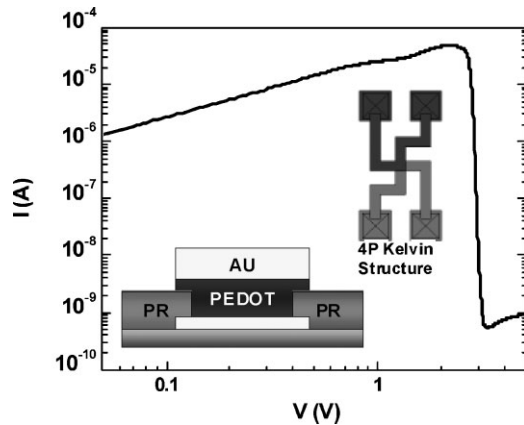


**Figure 1.** Typical current–voltage characteristics of a PEDOT/PSS fuse with 5  $\mu\text{m}$  diameter. The fuse interrupts at about 2 V. Fuse interruption does not depend on the polarity and hardly changes with scan speed. The inset shows the layout of the four-point probe Kelvin structure and a schematic cross-section of the fuse. The PEDOT/PSS is processed in vertical interconnects defined in the photoresist and sandwiched between top and bottom gold electrodes.

presented in Figure 2. The square gray areas are the top and bottom gold electrodes of the four-point probe Kelvin device layout. The round sphere in the middle is the vertical PEDOT/PSS interconnect. Upon fuse interruption, the interconnect literally blows up. Electron microprobe analysis showed only the presence of gold on the expanded surface of Figure 2a. This indicates that the PEDOT is still enclosed between the gold electrodes. To study the microstructure in more detail, focused ion beam (FIB) measurements were performed, and a cross-section of an interrupted fuse was made. The chemical composition as presented in Figure 2 was obtained from the secondary electron emission measured at a tilt angle of  $45^\circ$ . The Pt layers on top were deposited before milling to prevent charging. The bottom and top gold contacts show different dark and bright regions due to grains with a different crystallographic orientation. Figure 2 shows that the PEDOT/PSS layer is delaminated from the bottom gold contact. PEDOT/PSS only adheres to the surrounding photoresist. The void disconnects the top and bottom electrodes. The electrical discontinuity causes the large current drop in the current–voltage measurements. The volume change upon fuse interruption is clearly visible in an optical microscope. A representative movie is included in the supplementary information.

Fuses were made with PEDOT/PSS with different bulk conductivities. The device resistance depends on the type of PEDOT/PSS and varied between  $10^3 \Omega\mu\text{m}^2$  and  $10^8 \Omega\mu\text{m}^2$ . The device resistance is about two to three orders of magnitude higher than expected from the bulk conductivity. This difference is due to the contact resistance between PEDOT/PSS and the bottom gold electrode. The critical voltage and the critical power density for fuse interruption as a function of the fuse diameter are presented in Figure 3. The critical voltage is about 2 V, almost independent of fuse diameter and device resistance. The critical power, taken as the electrical power at fuse interruption, does not depend on the device diameter. The power varies between  $10^0$  and  $10^5 \text{Wcm}^{-2}$  depending on the bulk conductivity of PEDOT/PSS. Fuses with a surface area of about 10 to  $100 \mu\text{m}^2$  interrupt at a critical power as low as a few  $\mu\text{W}$ .

To estimate if fuse interruption is caused by a thermal process we use a simple static thermal model. The fuse is treated as a thin circular heating element with radius,  $a$ , on top of a Si substrate that acts as a heat spreader. When electrical power is dissipated in the fuse, the temperature rise over time is determined by the boundary conditions, dimensions, material properties of all

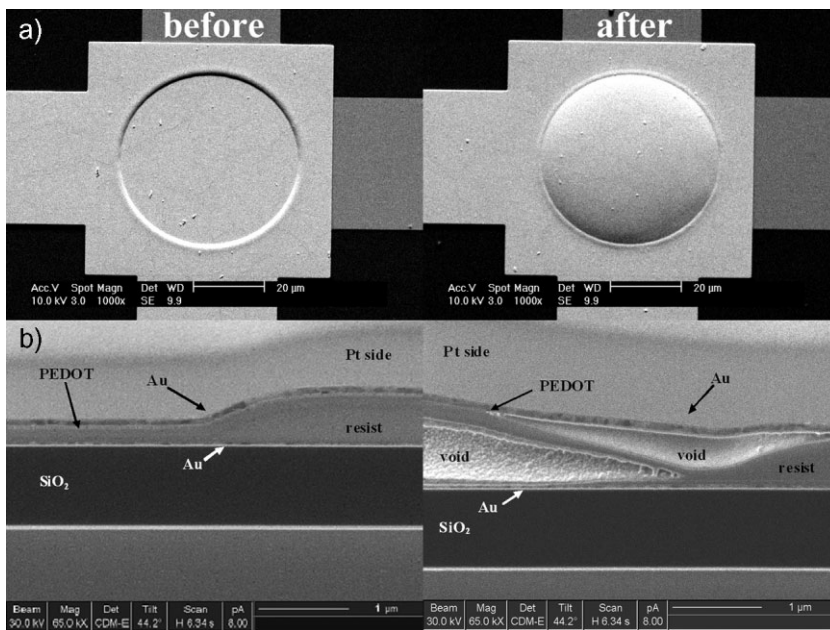


**Figure 2.** a) SEM photographs of a PEDOT/PSS fuse with a diameter of 50  $\mu\text{m}$  before and after interruption. The square gray areas are the top and bottom gold electrodes of the four-point probe Kelvin device layout. The round sphere in the middle is the vertical PEDOT/PSS interconnect. Upon fuse interruption, the interconnect is literally blown up. b) The cross-section was made using a FIB200 (Focused Ion Beam). First a thin layer of Pt is deposited to avoid charging. Then a 1.0  $\mu\text{m}$  Pt layer is deposited on the region of interest to protect the sample during FIB milling. A hole is milled using 30 keV Ga ions in the surface with one steep edge (oriented perpendicular to the sample surface) at the region of interest, and a step-like construction at the opposite side. In this way the cross-section is made and studied in the FIB at a tilting angle of  $45^\circ$ . Ga ions are used to scan the sample, and the image is formed by detection of the secondary electrons.

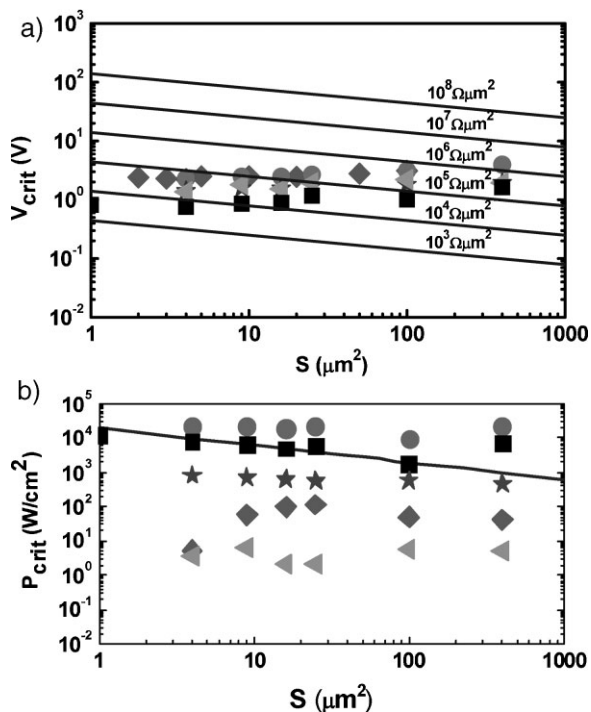


**Figure 3.** a) Critical voltage for fuse interruption as a function of fuse area. The solid lines are critical voltages as calculated for a simple static thermal model. b) Power at fuse interruption as a function of fuse area. The solid line is the critical power as calculated for a simple static thermal model.

layers involved, and time. As a first-order guess, we may consider a zero-thickness source with constant flux over its area on top of a semi-infinite substrate. For this case, the thermal resistance is given by:

$$R_{th} = 8 / (3\pi^2 ka) \quad (1)$$

where  $k$  is the thermal conductivity of the substrate.<sup>[6]</sup> The thermal power to reach a certain critical temperature,  $T_c$ , is equal to the temperature rise ( $\Delta T_c = T_c - T_0$ , with  $T_0 = 300$  K) divided by the thermal resistance. In this simple thermal model the fuse interrupts when the provided electrical power equals the thermal power. This equality yields the following expressions for the critical power and critical voltage:

$$P_c = 3\pi^2 ka \Delta T_c / 8 \quad (2)$$

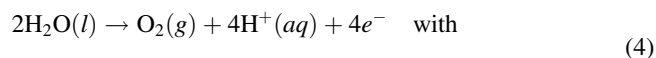
$$V_c = \sqrt{3\pi^2 ka \Delta T_c R / 8} \quad (3)$$

where  $R$  is the electrical fuse resistance.

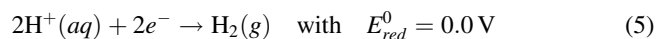
For an estimate, we take  $\Delta T_c$  of 100 K as a typical value for dedoping the conducting polymer, and we take a substrate thermal conductivity,  $k$ , of 120 W mK<sup>-1</sup>. The calculated values for critical voltage and critical power are included as the solid lines in Figure 3. There is no agreement between estimated and measured values. Apart from a discrepancy in the numerical

values, the functional dependences are exactly opposite as expected. In a simple thermal model the fuse interrupts when the delivered electrical power equals the critical thermal power. Hence, the critical electrical power should be independent of the device's electrical resistance, while the critical voltage is expected to increase with device resistance. We conclude that fuse interruption is not due to thermal dedoping. The inadequacy of a thermal explanation also follows from some additional runs that have been performed, including the gold and SiO<sub>2</sub> layers on top of the Si substrate attached to a chuck at room temperature. For example, the calculated temperature rise for a 100 μm<sup>2</sup> fuse dissipating 10<sup>3</sup> W cm<sup>-2</sup> was only 1 °C.

The critical voltages being constant and about 2 V strongly indicates that electrolysis of water in the PEDOT/PSS is responsible for fuse interruption. The oxidation and reduction electrode half-reactions are:<sup>[7]</sup>



$$E_{ox}^0 = -1.23 \text{ V}$$



At a pH of zero the reduction potential of water is 0 V by definition, and the oxidation potential is 1.23 V. Both electrode potentials depend on pH but shift in parallel.<sup>[8]</sup> Hence the potential for water electrolysis at 25 °C is 1.23 V at all pH's. However, a free energy of activation is often needed for the reaction to occur. Required overpotentials may easily amount to about 1 V.<sup>[9]</sup> Therefore, potential values for water electrolysis are typically around 2 V, which is comparable to the values of the critical voltages. Gasses formed upon hydrolysis cannot escape because the fuses are enclosed in the photoresist and sandwiched between a top and bottom electrode. The pressure rises and the fuse expands. The PEDOT/PSS delaminates at the least adhering surface, which Figure 2 shows is the bottom gold contact. To even further reduce the adhesion, self-assembled monolayers (SAMs) of alkanethiols were applied on the bottom gold electrode. However, no changes in critical voltage were measured.

Fuse interruption is a self-limiting process. Upon delamination the current path is interrupted and the electrolysis stops. The equivalent circuit of the fuses is represented by the PEDOT/PSS bulk resistance in series with the contact resistances, all shunted by the nonlinear resistance of the electrochemical cell. The tiny amount of charge needed to generate sufficient gas to blow up the fuse can be calculated from the expanded volume. The electrochemical current is a negligible fraction of the total current. The experimental data of Figure 3 can now be explained as follows: fuse interruption occurs at the onset of electrochemical decomposition of water, around 2 V, the current at fuse interruption is dominated by the PEDOT/PSS resistance, and the electrochemical current can be disregarded.

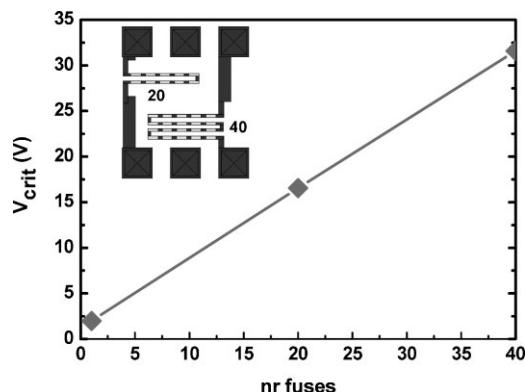


**Figure 4.** Critical voltage for breakdown of strings as a function of the number of interconnected fuses.

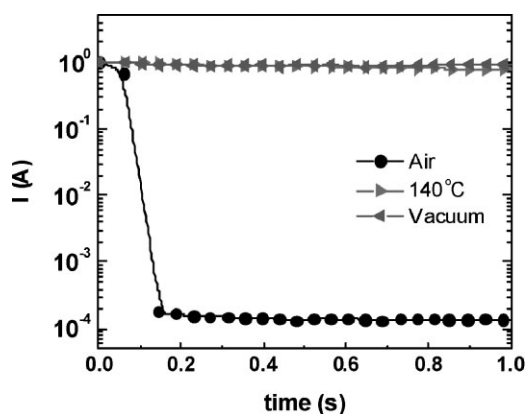


**Figure 5.** Current as a function of time. A constant bias of 2.5 V was applied. In air at room temperature the fuse interrupts at about 0.1 s. In vacuum and at a temperature of 140 °C, the fuses do not interrupt but are stable over time.

Figure 3 shows that the breakdown is voltage driven and not current driven. A threshold voltage for circuit interruption can be set by connecting fuses in series. Figure 4 shows that the critical voltage for interruption of strings linearly increases with the number of interconnected fuses.

Electrochemistry relies on the presence of water. To support electrolysis as the responsible mechanism, the fuse interruption was measured as a function of ambient pressure and temperature. A constant bias of 2.5 V was applied and the current was measured. Figure 5 shows the current as a function of time. At room temperature in air the fuse interrupts after about 100 ms. However, when the measurement is either done

in dynamic vacuum of  $10^{-5}$  mbar or in air at 140 °C, the fuse does not interrupt. The water content of the fuse is then too low. Changing the bias does not make a difference. The devices in vacuum or at elevated temperatures were stable up to at least 7 V. Finally we note that the operation is not limited to PEDOT/PSS. Fuses based on poly(vinyl alcohol) in ambient conditions did interrupt as well. However, the bias needed was high because the conductivity of poly(vinyl alcohol) is negligible. In vacuum the fuses were stable, similar to the PEDOT/PSS based fuses.

In summary, we have fabricated vertical PEDOT/PSS fuses on 150 mm wafers yielding 500 fuses at a time. The fuse is processed in vertical interconnects defined in the photoresist and sandwiched between top and bottom gold contacts. Fuses with diameters from 10 to 100  $\mu\text{m}$  can be programmed with power as low as a few  $\mu\text{W}$ . The operation mechanism is not power-driven thermal dedoping but delamination of PEDOT/PSS by gas formation upon electrolysis of water. The process is voltage-driven and fuse interruption starts at the onset of electrochemical reduction of water, which is about 2 V. The technology can be implemented in existing organic electronic process flow-charts yielding the first electrically programmable WORM organic memories.

Received: April 8, 2008

Revised: May 8, 2008

Published online: September 1, 2008

- [1] E. Cantatore, T. C. T. Geuns, G. H. Gelinck, E. van Veenendaal, A. F. A. Gruijthuijsen, L. Schrijnemakers, S. Drews, D. M. de Leeuw, *IEEE J. Solid-State Circuits* **2007**, *42*, 84.
- [2] K. Myny, S. Van Winckel, S. Steudel, P. Vicca, S. De Jonge, M. J. Beenhakkers, C. W. Sele, N. A. J. M. van Aerle, G. H. Gelinck, J. Genoe, P. Heremans, *IEEE ISSCC Dig. Tech. Pap.* **2008**, 290.
- [3] I. P. Atkins, (Raychem Ltd.), Electrical circuit interruption device, European Patent EP0115191, **1984**.
- [4] A. W. Marsman, C. M. Hart, G. H. Gelinck, T. C. T. Geuns, D. M. de Leeuw, *J. Mater. Res.* **2004**, *19*, 2057.
- [5] S. Möller, G. Perlov, W. Jackson, C. Taussig, S. Forrest, *Nature* **2003**, *426*, 166.
- [6] H. Carslaw, J. Jaeger, *Conduction of Heat in Solids*, 2nd ed., Oxford University Press, Oxford **1959**.
- [7] *Handbook of Chemistry and Physics*, CRC Press, Inc., Boca Raton, FL **1986**.
- [8] D. M. de Leeuw, M. M. J. Simenon, A. R. Brown, R. E. F. Einerhand, *Synth. Met.* **1997**, *87*, 53.
- [9] W. J. Hamer, R. E. Wood, in: *Handbook of Physics*, (Eds: E. U. Condon, H. Odishaw), McGraw-Hill, New York **1958**.